

10-14-1992

On the Origin of Electron-Beam-Induced-Current Contrast of Extended Defects in Silicon

M. Kittler

Institute of Semiconductor Physics

W. Seifert

Institute of Semiconductor Physics

Follow this and additional works at: <https://digitalcommons.usu.edu/microscopy>



Part of the [Biology Commons](#)

Recommended Citation

Kittler, M. and Seifert, W. (1992) "On the Origin of Electron-Beam-Induced-Current Contrast of Extended Defects in Silicon," *Scanning Microscopy*. Vol. 6 : No. 4 , Article 9.

Available at: <https://digitalcommons.usu.edu/microscopy/vol6/iss4/9>

This Article is brought to you for free and open access by the Western Dairy Center at DigitalCommons@USU. It has been accepted for inclusion in Scanning Microscopy by an authorized administrator of DigitalCommons@USU. For more information, please contact digitalcommons@usu.edu.



ON THE ORIGIN OF ELECTRON-BEAM-INDUCED-CURRENT CONTRAST
OF EXTENDED DEFECTS IN SILICON

M. Kittler * and W. Seifert

Institute of Semiconductor Physics
Walter-Korsing-Str. 2
D-O 1200 Frankfurt (Oder), Germany

(Received for publication January 23, 1992, and in revised form October 14, 1992)

Abstract

The paper reviews the origin of bright and dark Electron-Beam-Induced Current (EBIC) contrast due to extended defects in silicon, inclusively a brief discussion of contrast modelling. Particular emphasis is put on the role of impurities demonstrated to determine contrast in many cases (extrinsic contrast origin). The understanding of the prevalent contrast type - dark contrast due to enhanced recombination at defects - is well supported by existing phenomenological contrast models which can, therefore, be used as a basis for contrast interpretation. In the context of extrinsic vs. intrinsic contrast origin, the influence of defect dimensionality on contrast is addressed, indicating that grain boundaries of even low recombination activity might produce detectable contrast, in contradiction to dislocations and point-like defects. It is shown that transition-metal precipitates are very efficient recombination sites and that their activity is in accordance with the existence of internal Schottky barriers.

Key Words: Electron-beam-induced current, extended crystal defects, dislocations, stacking faults, grain boundaries, precipitates, dark and bright EBIC contrast, intrinsic and extrinsic EBIC contrast, diffusion length, semiconductor characterization, silicon

*Address for correspondence:

Martin Kittler

Institut für Halbleiterphysik, POB 409

D-O 1200 Frankfurt (Oder), Germany

Fax No: + 0335-326195

Introduction

Extended crystal defects such as dislocations, stacking faults, grain boundaries or precipitates often appear as EBIC contrast. Usually dark contrast, i. e. a reduced EBIC due to the defect action, is observed, but bright contrast - or bright haloes around defects - i. e. an enhanced EBIC due to defect action can be observed, too. Sometimes defects show no contrast at all even under favourable imaging conditions.

The local electrical properties leading to the EBIC contrast may be either intrinsic to the considered defect or may be caused by interaction with point defects/impurities. The first case will be called intrinsic contrast, the latter extrinsic contrast. There has been long discussion on this problem and at least for silicon, extrinsic origin seems to dominate in many cases.

The EBIC contrast contains information about electrical defect properties. Further, it depends on defect geometry (shape and position), on electrical properties of the material surrounding the defect (resistivity, lifetime, surface recombination ...), it is affected by the electron probe (beam energy E_0 , beam current I_b) as well as by the conditions of the sample (temperature, additional bias voltage to the collecting junction). For early experimental work relating to these aspects see e. g. Leamy et al. /32 / or /20 /.

The aim of this paper is a discussion of the causes of defect electrical activity and an interpretation of the defect action from the point of view of solid state physics. This can give important information for device technology helping to keep the defect action under control.

In the following, the contrast mechanisms of dark and bright contrasts will be analyzed. Because interaction of point defects (impurities) with extended defects plays an important role for the formation of EBIC contrast, a brief discussion concerning this topic will be given first.

Interaction of Impurities with Extended Defects

Impurities in Si to be taken into account are:

- transition metals (TM), especially Fe, Cu, Ni, which are mainly introduced by contamination during technological treatments,
- oxygen, especially in the case of Czochralski silicon (CZ) which is introduced during crystal growth from the melt,
- dopants as B, P, As ...

Solubility, diffusivity as well as concentration of these species strongly influence the interaction with the extended defects.

The total concentration of TM in the as-grown material is below 10^{12} cm^{-3} . However, during technological treatments, the concentration can increase up to 10^{14} cm^{-3} or even more. TM are highly mobile and their solubility in the silicon lattice is large at high temperatures. Changing the temperature from values typical for technological treatments (around $1000 \text{ }^\circ\text{C}$) down to room temperature the solubility decreases by orders of magnitude. Consequently, TM become supersaturated then and precipitate or form complexes /16/. In the case of Cu and Ni, for instance, a very large amount of atoms precipitate homogeneously as silicides (Cu_3Si , NiSi_2) /42/. On the other hand, Fe precipitates mostly heterogeneously, when extended defects are available. A large amount of Fe remains in solution during cooling and forms FeB-pairs if the silicon material is doped with boron. For more detailed information see e. g. /15/.

Oxygen is introduced during CZ crystal growth, in a concentration of $10^{17} \dots 10^{18} \text{ cm}^{-3}$. During heat treatments, oxygen may precipitate as SiO_x particles and form thermal donors /5/ which influence the resistivity or even change the conductivity from p- to n-type silicon.

Dopants are introduced in the crystal intentionally to define conduction type and resistivity. They have a very high solubility and can be found in concentrations up to around 10^{19} cm^{-3} . Typically, material with a doping concentration in the range of $10^{14} \dots 10^{15} \text{ cm}^{-3}$ is used. Among the dopant atoms, phosphorus has a quite large segregation coefficient.

Capture and binding of impurities by extended defects take place during cooling down from high temperatures, see e.g. /49/ or /47/. Different mechanisms may be responsible for this. Elastic forces result from the deformation of the crystal lattice and are known, for instance, to lead to Cottrell atmospheres at dislocations. Such forces can exist around precipitates, also. Chemical bonding or saturation of dangling bonds by extrinsic atoms and Coulomb interaction between impurities and charged defects are other possibilities.

All the mechanisms act only over a short distance. So, impurities must first arrive in the vicinity of the extended defects before they can be captured. The transport of impurities is determined by the diffusivity which is large for TM and small for dopants or oxygen /44/. Consequently, TM may play a dominating role for decoration of extended defects.

When considering the interaction of impurities with extended defects, one must not forget to take into account the balance between total concentration of impurities in the material studied and the density of capture centres/getter sites, which is related to density, type and dimension of the extended defects. Having a given concentration of impurities, the intensity of decoration of the extended defects may increase with decreasing density of getter sites and vice versa.

EBIC is a useful tool for studying such interactions of impurities with extended defects. In particular, examples of bright EBIC contrast have very clearly demonstrated this. Some of them will be discussed in the next section.

Bright EBIC Defect Contrast

Bright contrast at extended crystal defects in silicon is a rather occasionally observed feature, but, nevertheless, has gained increasing interest recently. Its explanation is difficult sometimes since different mechanisms may be involved in contrast formation and a theoretical modeling has not yet been performed.

In general, when considering possible causes of bright contrast, one has to distinguish between

- direct electronic effect of charges at defects on minority carriers, i. e. intrinsic defect contrast and
 - indirect defect action due to defect-induced redistribution of extrinsic point defects in the defect surrounding, i. e. extrinsic defect contrast.
- Observations on bright defect contrast are discussed in a few papers; for Si see e. g. /19, 4, 2/ and for compound semiconductors see e. g. /11, 12/.

Bright contrast due to extrinsic origin

Bright haloes around defects and sometimes sole bright contrasts may result from defect-induced redistribution of point defects. The contrast can be caused by both inhomogeneities of recombination properties and inhomogeneities of net doping leading to variations of the width of the collecting space-charge layer.

Bright contrast due to zone of reduced recombination. In the neighbourhood of decorated crystal defects, zones of bright contrast may be observed due to reduced recombination, i. e. enhanced diffusion length (DL) of minority carriers, which results from the denudation of

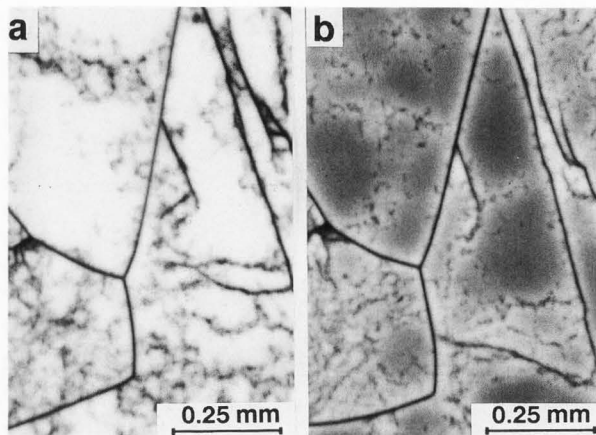


Fig. 1: EBIC micrographs ($E_0 = 30$ keV, beam current < 100 pA) of a polycrystalline silicon sample before (a) and after furnace annealing (b).

recombination active impurities within so-called *getter zones*. Under appropriate conditions, variations of the DL by only a few percent are easily detectable. Examples of bright contrast caused by gettering of recombination-active impurities are given in many papers: for dislocations see e. g. /3/, for grain boundaries (GB) e. g. /35/.

Fig. 1 compares EBIC contrasts of defects in polycrystalline Si before and after heat treatments. As a result of the heat treatment, bright getter zones appeared with widths depending on cooling rate /28/. Taking into account extension and strength of both bright zone around and dark contrast at GB's, as revealed by EBIC profiles, the total effect of certain GB's was found to be an increase of charge collection. This observation might be interpreted as transformation of impurities into a less recombination-active state when occupying the grain boundaries.

Bright contrast due to inhomogeneities of doping. Depending on the experimental conditions, both enhanced and decreased doping concentration may lead to bright contrast. The effect was first reported for dopant striations in /32/ and is due to a modulation of width w and electrical field strength E of the collecting junction:

$$w \propto N^{-1/2} \quad (1)$$

and

$$E \propto N^{1/2} \quad (2)$$

with N the net doping concentration.

Fig. 2 presents results obtained on oxygen-induced defects in initially p-type silicon (200 Ωcm) annealed for 20 h at 1100 $^{\circ}\text{C}$. After thermal-donor (TD) formation at 450 $^{\circ}\text{C}$, the sample became n-type and bright contrasts were found for $E_0 > 15$ keV (Fig. 2a). On the other hand, with the thermal donors

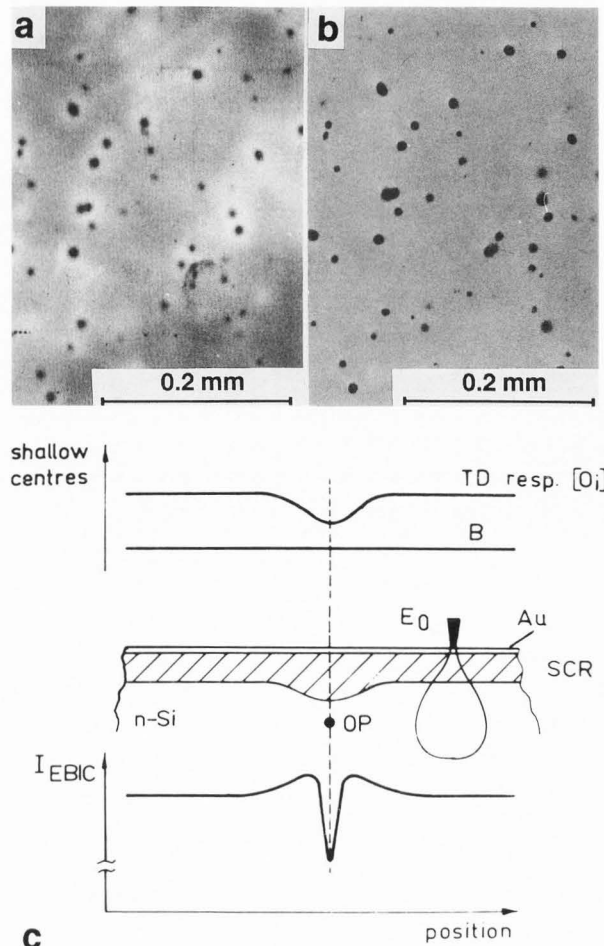


Fig. 2: EBIC contrast ($E_0 = 30$ keV) at oxygen induced defects: a) after thermal donor (TD) formation, b) after TD destruction, c) schematic illustration.

destroyed, only dark contrasts were observed (Fig. 2b). The contrast mechanism is illustrated in Fig. 2c: The net doping level after 450 $^{\circ}\text{C}$ annealing is defined by the concentration of the thermal donors. The bright contrast is due to a reduced TD concentration causing a larger width of the junction space-charge region (SCR) according to relation (1). The TD concentration in turn reflects the denudation of interstitial oxygen around the defect /43/. This interpretation is supported by a good correspondence between dimensions of bright zones and diffusion length of oxygen.

The second case of doping contrast may be observed at low beam energies and high injection when the generation volume is inside the junction space-charge region and a relatively stable electron-hole plasma is formed. Under these conditions the electrical field strength E of the junction determines the efficiency of charge

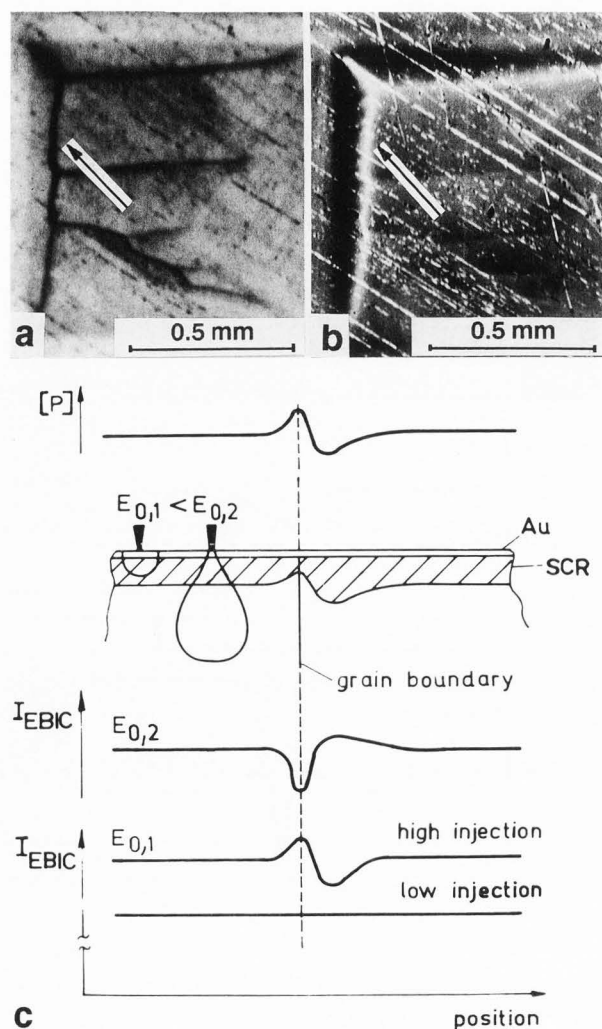


Fig. 3: Bright contrast due to enhanced doping concentration at grain boundaries in a SOI layer: a) $E_0 = 30$ keV, low injection; b) $E_0 = 5$ keV, high injection; c) schematic illustration.

collection, thus regions of higher doping give a larger EBIC signal because of stronger electrical field-see relation (2). Fig. 3 demonstrates this behaviour for grain boundaries in a thick phosphorus-doped Silicon-On-Insulator (SOI) layer, for details see /27/. The dramatic contrast change at the grain boundaries (GB's), see arrow in Fig. 3, is a clear indication of this contrast mechanism and shows that the near surroundings of the bright GB's are enriched with dopants. This explanation (Fig. 3c) agrees nicely with results of detailed considerations of the recrystallisation process which indicate that the GB's in question are sites where two solidification fronts have met and segregation effects of phosphorus could be strong /27/.

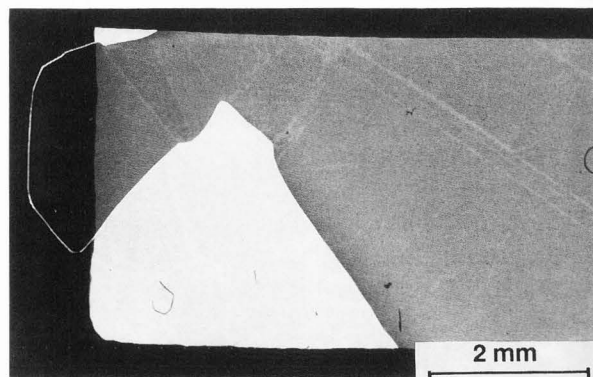


Fig. 4: Bright contrast due to charge collection at a grain boundary outside the Schottky contact area ($E_0 = 30$ keV).

Bright contrast due to intrinsic origin

Charged defects may exert an attractive or repulsive force on electron-beam-generated minority carriers, depending on the charge sign.

(a) A repulsion of minority carriers can take place when defects are charged with carriers of the same sign. Depending on the geometrical situation, an enhanced or decreased EBIC signal is expected then. Evidence that this type of contrast mechanism is acting at CuSi lamella in p-type Si was presented in /13/.

(b) The case of minority carrier collection by the space charge around defects and transport of the collected carriers inside the defect was recently reported. Kolbe et al. /31/ reported bright contrast of GB's and dislocation loops in n-type Si. Gleichmann et al. /14/ found bright contrast at small angle GB's arising at the interface of two bonded wafers. Fig. 4 shows an example for bright contrast of a GB outside the Schottky contact area in p-type Si. The effect was first observed at low temperatures (90 K), but can be found at room temperature, too. It is interpreted as minority carrier collection at the GB's, followed by charge carrier transport to the Schottky contact.

Further origin of bright defect contrast and summary

Extended defects located in reverse-biased SCR's of p-n junctions may cause inhomogeneities of the electrical field, leading to charge carrier multiplication (microplasma). As a result the EBIC increases and the corresponding defect becomes visible as bright microplasma contrast. Examples are given e.g. in /39, 17, 24/.

Preferentially etched defects may show bright topography contrast in EBIC, compare e. g. Fig. 6. The microtopography is believed to modify the primary beam energy absorbed in the semiconductor in such a way, that the number of generated electron-hole pairs is increased.

For further types of bright contrast see e. g. /29/. Because of the variety of existing contrast mechanisms, the interpretation of bright contrast is difficult. However, a lot of the examples given for the bright defect contrast demonstrate clearly the interaction of extended defects with impurities: for example with recombination-active impurities in the case of bright getter zones (Fig. 1), with oxygen in the case of bright haloes around oxygen precipitates (Fig. 2) or with phosphorus in the case of GB's in a SOI layer (Fig. 3). Interaction of Fe with extended defects, leading to bright areas in EBIC under appropriate experimental conditions, is analyzed in /26/.

Dark EBIC Defect Contrast

General Remarks

Dark contrast due to *enhanced recombination* is the common contrast type and has been observed for all kinds of extended defects. During the last decade, since the pioneering work of Donolato /6/, significant progress has been made in modeling such recombination contrast. While contrast theory was limited to weak defects initially /6, 7/, strong defects are considered nowadays as well, see /37, 8, 38, 9/.

All contrast models are, essentially, solutions of the diffusion equation for a certain sample geometry used in EBIC experiments, with the defect assumed to be a region of decreased minority-carrier lifetime, i. e. enhanced recombination. The physics of recombination at the defect is not considered.

Within the first-order approximation the contrast of a defect $c = (I_0 - I_d)/I_0$ can be written

$$c = G \cdot F \tag{3}$$

with G the recombination strength of the defect and F a factor which can be calculated on the basis of the considered contrast model (I_0, I_d currents collected far away or at the defect, respectively). In particular, for point-like defects, one has $c = \gamma \cdot f$, with γ in μm and f in μm^{-1} , for line-shaped defects $c = \Gamma \cdot F$, G and F dimensionless, /21, 22/, and for planar defects there holds $c = g \cdot \mathcal{F}$, with g in μm^{-1} and \mathcal{F} in μm .

It is worth briefly discussing an interesting property of the strength of a small spherical defect which will be referred to later. In the first-order approximation, the defect strength γ is given by

$$\gamma = (4\pi/3) \epsilon^3 (L_d^{-2} - L^{-2}) \tag{4}$$

ϵ being the radius of the defect, L_d the diffusion

length inside the defect region and L the diffusion length in the surrounding of the defect. This first-order strength γ increases when L_d decreases.

Recently, it has been shown that there exists an upper limit of the strength of a small spherical defect /9/ given by

$$\gamma = 4\pi \epsilon \tag{5}$$

This means that even if $L_d \rightarrow 0$, that is, if the carriers reaching the defect recombine immediately (defect acts as 'black hole'), the recombination flux is finite. A further implication of (5) is that a certain experimental contrast value requires a certain minimum defect radius. Thus, there is a possibility to estimate the radius of the electrical action of the defect.

Despite several simplifying assumptions, contrast modeling according to /6/ was found to produce sufficient results in interpreting experimental contrast data /25/. This is true for defects in the neutral semiconductor. Theoretical modeling for defects in the junction space charge region has recently been developed /46, 48/. It has to be emphasized that the physics of recombination is not the subject of the theories considered here. This means that the data we get are of only phenomenological nature and do not allow conclusions about origin of recombination. Variation of additional physical parameters as e. g. sample temperature T and beam current I_b /50/ or junction bias U_{bias} /10/ can help to get this insight, provided the contrast models are supplemented by corresponding physical models of recombination at defects.

Before discussing experimental results, let us consider the influence of defect dimensionality on contrast. Assume the following arrangements of dislocations (Fig. 5):

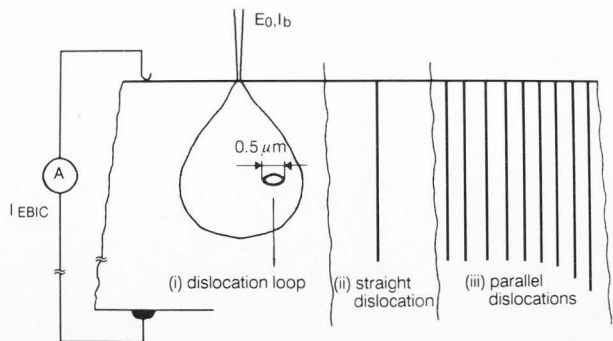


Fig. 5: Different arrangements of dislocations standing for point-like (a), line-shaped (b) and planar (c) defects.

(a) a small dislocation loop of 0.5 μm diameter at optimum depth for producing maximum EBIC contrast,

(b) a straight dislocation perpendicular to the surface, and

(c) a set of parallel dislocations of 0.5 μm distance lying in a plane perpendicular to the surface.

The small loop can be considered a point-like defect for beam energies > 30 keV as the diameter of the generation volume in Si ($> 6 \mu\text{m}$) is much larger than the defect diameter then. The array of parallel dislocations (c) stands for a small-angle grain boundary, i. e. a planar defect.

Assuming now, in all three cases for the dislocations, an identical recombination strength Γ and using first-order theory /6/, one calculates for a beam energy $E_0 = 30$ keV and a diffusion length $L = 100 \mu\text{m}$ in case (a) $c = 0.04 \Gamma$ (this maximum contrast is formed when the small loop is in a depth of about $4 \mu\text{m}$), in case (b) $c = 0.18 \Gamma$, and in case (c) $c = 6.4 \Gamma$. Consequently, for the given situation, the relation of the contrasts is 1 : 4.5 : 165. Thus, planar defects (grain boundaries) need a much lower recombination activity than line-shaped or point-like defects to produce a certain contrast value.

In analogy to point-like and line-shaped defects /22/, the EBIC contrast of a planar defect can be written in the form

$$c = (\vartheta \sigma v_{th} / D) \cdot \mathcal{F}(R, L; \text{geometry}) \quad (6)$$

or

$$c = (s / D) \cdot \mathcal{F}(R, L; \text{geometry}) \quad (6^*),$$

with ϑ the number of recombination centres per unit area, σ their capture cross section for minority carriers, v_{th} the thermal velocity, D the minority carrier diffusivity, s the surface recombination velocity, and \mathcal{F} a factor which is easily calculated for a particular defect and depends on electron range R , diffusion length L and defect geometry. For a grain boundary perpendicular to the surface, a diffusion length of $100 \mu\text{m}$ and a beam energy of 30 keV, one calculates $\mathcal{F} = 3.2 \mu\text{m}$.

The minimum surface recombination velocity s_{min} a grain boundary must have to produce detectable contrast is

$$s_{min} = c_{min} D / \mathcal{F} = 1.5 \cdot 10^2 \text{ cm s}^{-1}$$

if $D = 10 \text{ cm}^2 \text{ s}^{-1}$ and $c_{min} = 5 \cdot 10^{-3}$ are taken. With $v_{th} = 10^7 \text{ cm/s}$ this corresponds to the following density of centres when $\sigma = 10^{-15} \text{ cm}^2$ is assumed:

$$\vartheta_{min} = s_{min} / \sigma v_{th} = 1.5 \cdot 10^{10} \text{ cm}^{-2}.$$

Both relations (6) and (6*) and estimation of contrast relation between defects of different dimensionality

are based on linear approximation. Although this approximation is not generally applicable, it allows satisfactory modeling of weak contrast and can therefore be applied to draw the above conclusions.

Origin of dark contrast

The question about the origin of dark contrast can not be answered by the contrast models mentioned above. Nevertheless, they can support the understanding of contrast origin.

From experience, it seems that the intrinsic recombination strength of dislocations in Si is too small to form visible contrast (e. g. /45/). This might not be the case for grain boundaries according to the above estimations. So, dislocations and grain boundaries (as well as stacking faults) will be discussed separately. Finally, dark contrasts of metal silicide particles will be analyzed.

Dark contrast of dislocations. A lot of experimental results indicate that one and the same dislocation type can be with or without dark EBIC contrast. The contrast values are often found to be strongly dependent on heat treatments. In other words, the crystallographic type of the dislocation does not unambiguously define the recombination strength, in contrast to former assumptions by a number of researchers.

Fig. 6 clearly demonstrates this message for dislocations bounding epitaxial stacking faults (for details see /23/). In the as-grown samples, all defects were without recombination contrast, the only contrast being bright EBIC topography contrast caused by preferential etching of the defects. After a heat treatment or even after storage of the untreated samples for some months at room temperature, a part of the bounding partial dislocations exhibited dark recombination contrast while other crystallographically identical bounding partials did not. The stacking fault planes were without contrast in all cases. It was observed that the probability of a dislocation to show dark contrast after annealing is dependent on the dislocation type. The higher b^2 ($b =$ Burgers vector), i. e. the perturbation of the lattice, the higher was the probability of dark contrast.

These findings clearly support the view that dislocation contrasts are strongly influenced by interaction with impurities. However, no impurities (precipitates) could be detected at the active defects using TEM. This 'disagreement' is eliminated by a theoretical estimation according to which a very small amount of recombination-active impurities is sufficient to produce clearly visible EBIC contrast: For instance a few hundred recombination centres per μm dislocation length, with a capture cross-section for minority carriers of 10^{-14} cm^2 , are sufficient for detectable contrast /22/. Another example for the important role of impurities is presented in Fig. 7. Here, the recombination activity

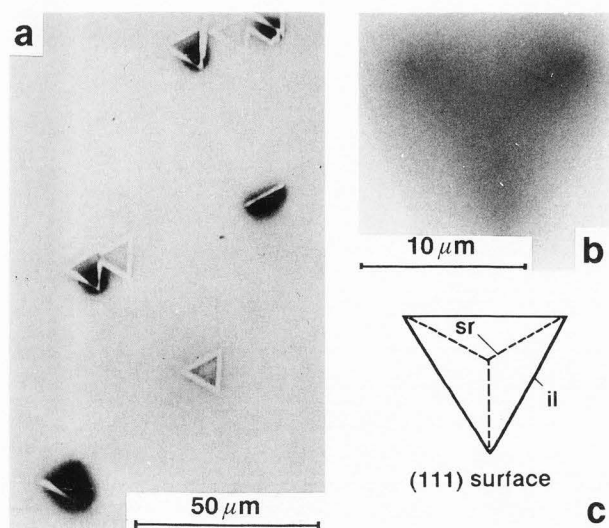


Fig. 6: EBIC contrast of epitaxial stacking faults: a) overview ($E_0 = 20$ keV); b) detail ($E_0 = 30$ keV), demonstrating activity of partial dislocations; c) illustration of stacking fault geometry (sr: stair-rod partial dislocation, il: intersection line between stacking fault and surface).

of dislocations in a polycrystalline sample is strongly reduced due to annealing.

Recently misfit dislocations at the interface between a Si substrate and a Si(2%Ge) epi-layer were studied by Rozgonyi and co-workers /33/. The misfit dislocations were found without contrast in the as-grown state, but appeared in dark contrast after annealing. An intentional contamination with metals (Cu, Ni, Au) produced a marked contrast, being of dotted character for Cu and Ni. This was attributed to Cu and Ni silicides decorating the dislocation lines.

All these observations clearly emphasized the important role of impurities for the formation of dark EBIC contrast of dislocations in Si. Thereby, already a small accumulation of recombination-active impurities, not yet detectable by analytical methods, is assumed to be sufficient to form contrast. Metal silicide precipitates decorating the dislocations, might be responsible for the formation of strong recombination contrast.

Dark contrast of grain boundaries. Most of the grain-boundary studies indicate that dark contrast at grain boundaries (GB's) results from impurities or imperfections in the boundary plane:

Battistella and Rocher /1/ found GB's in bicrystals without contrast in the as-grown state. After a heat treatment, the GB's appeared with dark dotted contrast. In a study of Maurice et. al. /35,36/ homogeneous EBIC contrast of GB's was visible in the as-grown state already, but annealing led to a marked increase of contrast which could be related

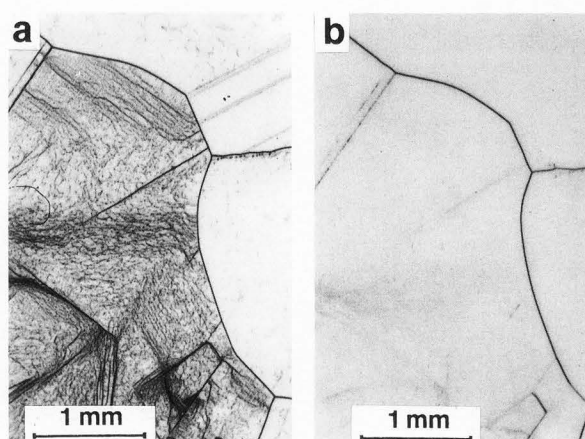


Fig. 7: Effect of annealing on recombination activity of dislocations in a polycrystalline Si sample ($E_0 = 30$ keV, parallel samples of nearly identical defect structure): a) before annealing, b) after annealing.

to Cu and Ni silicide particles by Transmission Electron Microscopy (TEM).

Our own studies of GB's in polycrystalline Si revealed a wide range of recombination activity in the as-grown state depending on the structure of the boundary. Annealing left the contrast of strongly active GB's practically unchanged whereas the contrast of less active twin boundaries disappeared. At certain GB's, clear evidence for space-charge regions was obtained by the technique of Matare and Laakso /34/ or from observations of charge collection at GB's outside the Schottky contact area (see Fig. 4) /28/. The same GB's showed strong dark contrast when investigated with the standard EBIC technique. This is a hint that space charge regions may contribute to the recombination activity of GB's. Correlated EBIC and TEM investigations established that GB's of high perfection have low contrast and general GB's with high density of dislocations in the boundary plane exhibit high recombination activity. Fig. 8 shows such a situation: a GB with strong contrast and a twin boundary with weak contrast. Using TEM, the GB was found decorated with precipitates, probably Cu silicide particles as concluded from the Moire fringes observed. The small contrast of the twins is in agreement with the experimental fact that stacking fault planes are usually without contrast, even in material having been subjected to strong temperature load. Fig. 9 demonstrates this for an oxidation-induced stacking fault (SF) bounded by a recombination-active Frank partial dislocation. There is no evidence for recombination activity of the fault plane. This may be understood as follows. The intrinsic recombination activity of the SF plane

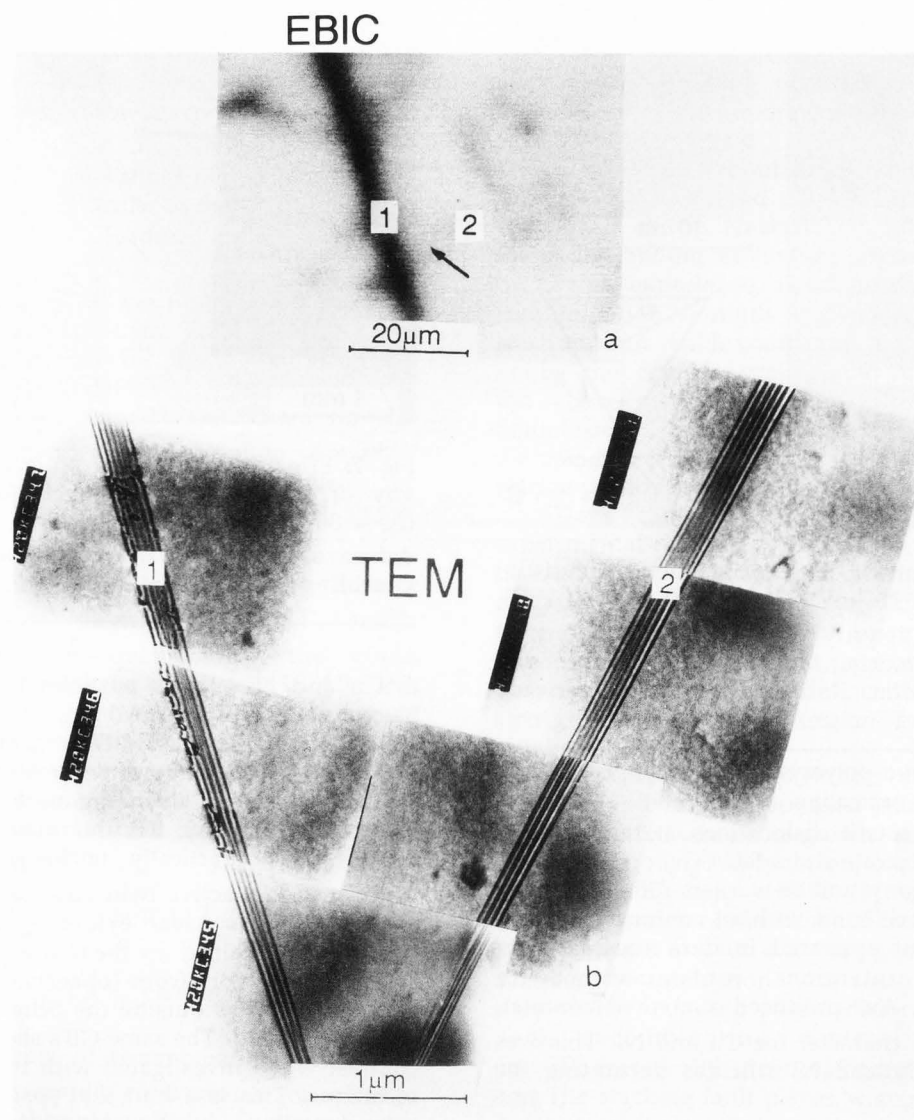


Fig. 8: 1:1 correlation of EBIC and TEM of a polycrystalline silicon sample:
 1 - GB with strong EBIC contrast,
 2 - twin boundary of low contrast

is small because of the weak deviation from the regular lattice structure. The interaction of the SF plane with impurities is small for the same reason, too. Consequently, the SF planes occupying a relatively small area as compared to a GB are free of EBIC contrast mostly while highly perfect twin boundaries may have a chance to produce a weak contrast due to their larger dimension.

Dark contrast of metal silicide particles. Metal silicide precipitates (MSP's) have been found to be strong recombination sites producing EBIC contrasts

of up to some 10 percent (Fig. 10). In case of Cu and Pd, the silicide precipitates are usually accompanied by secondary defects (dislocations, stacking faults) /40/. So it is difficult to judge about activity of the only precipitate.

The NiSi_2 precipitates, however, could be prepared as individual particles /41/, thus allowing investigations of their electrical activity without interference of other defects. It has been established for n-type silicon ($P = 4 \cdot 10^{14} \text{ cm}^{-3}$) that even small NiSi_2 particles of about $0.5 \mu\text{m}$ diameter and less than 20 nm thickness exhibit extraordinarily strong EBIC contrasts of up to $c = 0.4$ which corresponds to recombination strengths $\gamma \geq 15 \mu\text{m}$ /30/. The possible reason for this very

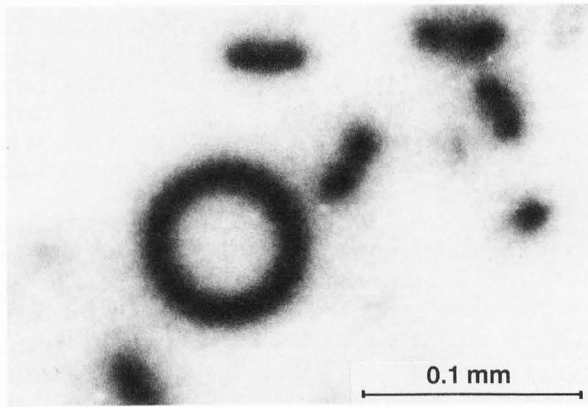


Fig. 9: EBIC micrograph of oxidation-induced stacking fault in p-Si ($E_0=30$ keV).

large recombination activity might be a depletion region around the particles which could strongly increase the effective capture cross-section of the defect for minority carriers. In fact, bearing in mind that the Schottky barrier height on n-type Si (111) is 0.79 eV for type-B and 0.65 eV for type-A NiSi_2 space-charge regions of the order of $1 \mu\text{m}^1$ are to be expected for the material studied.

This interpretation is confirmed by relation (3) requiring a defect radius of at least $1.2 \mu\text{m} / 9$ for the defect strength $\gamma = 15 \mu\text{m}$. The estimation demonstrates that the 'electrical radius' of these defects is much larger than the precipitates and is in agreement with the expected dimension of the depletion region. Consequently, our experimental results are a strong hint that MSP's may produce internal Schottky barriers which lead to a large increase of minority-carrier capture and to transport of the carriers to recombination centres located at or near the precipitate/matrix interface.

Let us discuss the influence of such defects on average DL now. If one describes the MSP as a 'black hole' of radius ϵ , then the minority carrier flux into an isolated MSP is $4 \pi D \epsilon p_0$, with p_0 being the minority carrier concentration far away from the defect. For a certain density of precipitates, N_{pr} , the recombination flux per unit volume is roughly given by:

$$I_{rec} = 4 \pi D \epsilon p_0 N_{pr} \quad (7)$$

With $\tau = p_0 / I_{rec}$, this leads to

$$\tau_{pr} = (4 \pi D \epsilon N_{pr})^{-1} \quad (8)$$

1) rough estimation based on a one-dimensional scheme for calculating SCR width

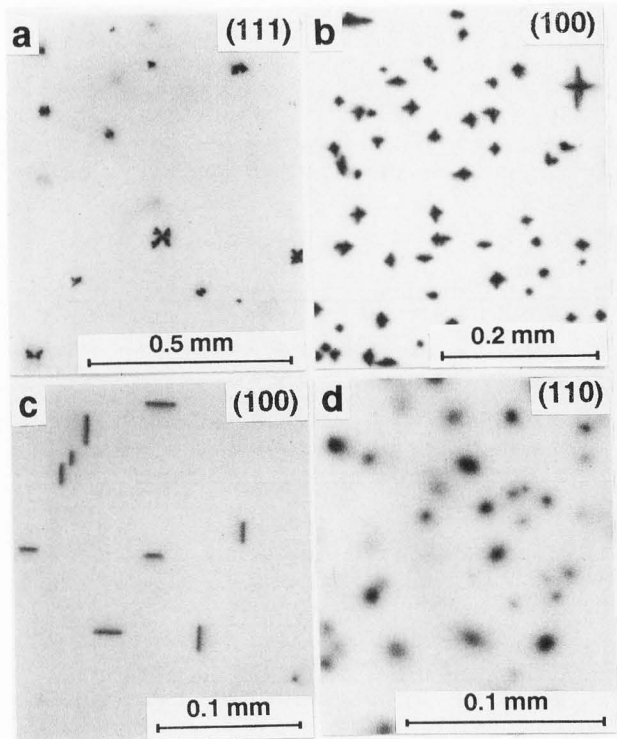


Fig. 10: EBIC contrast at metal-silicide particles: - star-shaped contrasts ($E_0=30$ keV) due to colonies of silicide particles and dislocations - (a) Cu silicide, (b) Pd silicide; - line-shaped contrasts ($E_0=20$ keV) due to large NiSi_2 platelets parallel to (111) planes (c); - point contrasts ($E_0=30$ keV) due to small NiSi_2 platelets

Table 1: Comparison of measured $/30/ (L_{exp})$ and estimated (L_{est}) DL in four different n-Si samples containing small NiSi_2 precipitates

$N_{pr} (\text{cm}^{-3})$	$L_{exp} (\mu\text{m})$	$L_{est} (\mu\text{m})$
$2 \cdot 10^8$	12.3	13
$6 \cdot 10^8$	8.4	7.4
$7 \cdot 10^8$	9.0	6.8
$8 \cdot 10^8$	7.2	6.4

The estimation of DL was based on formula (9) taking $\epsilon = 1.2 \mu\text{m}$ and $D = 10 \text{ cm}^2\text{s}^{-1}$.

or

$$L_{pr} = (4 \pi \epsilon N_{pr})^{-1/2} \quad (9)$$

The assumption made for obtaining this formula are large distances and absence of recombination between precipitates. Although this might not be fulfilled exactly, relation (9) gives a useful rough estimate of DL.

A comparison between estimated and measured DL is presented in Table 1. It demonstrates

a satisfactory agreement and is another argument for the developed picture of recombination activity of MSP.

Finally, it should be pointed out that the electrical action of MSP's is expected to depend on barrier height, Fermi level position and charge of the particle. The latter was demonstrated for oxygen precipitates /18 /already which are known to be positively charged.

Summary and Conclusions

The results presented above show that interaction with impurities plays a large role for the electrical activity of extended defects as observed by EBIC. This is clearly visible in case of certain bright contrast effects (e.g. getter zones) and can also be deduced from the dependence of contrast on thermal treatments. So, crystallography alone does not unambiguously define defect properties and extrinsic contrast origin seems to prevail in most cases.

Detectable EBIC contrast requires a certain minimum defect strength which is relatively high for point-like and line-shaped defects and makes intrinsic contrast origin unlikely. Contrarily, large planar defects such as grain boundaries have the chance to produce EBIC contrast even for low activity per unit area (surface recombination velocity around 100 cm s^{-1}).

As a rule, thermal treatments enhance the recombination activity of defects as impurities can be collected at the defect then. It is, however, not clear whether the increase of defect contrast is due to atmospheres of impurities with known electronic states, or due to interaction with the defect core and formation of new electronic states or due to formation of foreign phases and space-charge regions. The opposite effect, i.e. decrease of activity after thermal treatment, is possible, too, and has been found in polycrystalline silicon subjected to a rapid thermal annealing.

There are several indications that precipitates may strongly contribute to defect activity. In fact, precipitates of transition metals have been found to possess extraordinarily high recombination activity. Thus, small precipitates at dislocations, stacking faults and grain boundaries might lead to significant EBIC contrast. This has often been proved by EBIC/TEM correlations. Space-charge regions due to an internal Schottky junction seem to be responsible for the high recombination activity of metal silicide precipitates (MSP's) and the low diffusion length observed in material containing MSP's. It was found that the 'electrical radius' of the MSP's is much larger than the precipitate radius and close to the expected width of the Schottky depletion layer. Consequently, the space charge region and not the precipitate itself determines recombination activity, at least in an indirect way by providing a site for

accumulation of recombination-active impurities. The diffusion length data support this picture. SCR's have been shown to exist at certain grain boundaries (GB's) too, and to collect minority carriers very efficiently. As the same GB's showed strong dark contrast in usual Schottky barrier arrangement, it is quite natural to expect a dependence of contrast on barrier height.

The presented results on contrast of MSP's and GB's emphasize the importance of SCR's for electrical activity of defects. The details of recombination at MSP's and other extended defects (GB's) with SCR's are, however, not yet clear and require continuation of investigations by electron microscopic and electrical methods as well as physical modeling of recombination.

Acknowledgements

The authors would like to thank Dr. M. Seibt for supplying samples containing metal silicide precipitates, Mrs. G. Morgenstern for the TEM investigations of polycrystalline silicon and Mrs. M. Schultze for help in preparing the manuscript. Parts of this work were supported by the Bundesministerium für Forschung und Technologie, Bonn under contract No. 0329107F and by the Volkswagen-Stiftung under contract No. I/66 794.

References

- /1/ Battistella F, Rocher A (1987) Quantitative SEM/EBIC studies of carrier recombination in silicon bicrystals. *Semiconductor Science and Technology* **2**, 226-232.
- /2/ Blumtritt H, Kittler M, Seifert W (1989) On the formation of bright EBIC contrasts at crystal defects. *Inst. Phys. Conf. Ser., Inst. Physics - Bristol UK*, **104**, 233-238.
- /3/ Blumtritt H, Gleichmann R, Heydenreich J, Johansen H (1979). Combined scanning (EBIC) and transmission electron microscopic investigations of dislocations in semiconductors. *Phys. stat. sol. (a)* **55**, 611-620.
- /4/ Bode M, Jakubowicz A, Habermeier H-U (1986) Defects related to nitrogen implantation in silicon single crystals. *Diffusion and Defect Data* **48**, 21-28.
- /5/ Claeys C, Vanhellemont J (1989) Advances in the understanding of oxygen and carbon in silicon. *Solid State Phenomena, Vols. 6 & 7*, 21-32.
- /6/ Donolato C (1978/79) On the theory of SEM charge-collection of localized defects in semiconductors. *Optik* **52**, 19-36.
- /7/ Donolato C (1979) Contrast formation in the SEM charge-collection images of semiconductor defects. *Scanning Electron Microscopy, 1979; I*, 257-274.
- /8/ Donolato C (1983) Theory of beam induced current characterization of grain boundaries in silicon. *J. Appl. Phys.* **54**, 1314-1322.

- /9/ Donolato C (1992) A theoretical study of the charge collection contrast of localized semiconductor defects with arbitrary recombination activity. *Semiconductor Science and Technology* **7**, 37 - 43.
- /10/ Fell T S, Wilshaw P R (1989) Recombination at dislocations in the depletion region in silicon. *Inst. Phys. Conf. Ser.*, Institute Physics - Bristol UK, **104**, 227 - 232.
- /11/ Frigeri C (1989) On the nature of the impurity atmosphere around dislocations in bulk n-type GaAs. *Materials Science Forum*, Trans Tech Publications - Switzerland, Vols. **38-41**, 1379 - 1384.
- /12/ Frigeri C, Breitenstein O (1990) Influence of shallow donors on the formation of gettering regions in Czochralski GaAs. *Defect Control in Semiconductors*, K. Sumino (ed.), Elsevier Science Publ. (North Holland), 685 - 690.
- /13/ Gleichmann R, Blumtritt H, Heydenreich J (1983) New morphological types of CuSi precipitates in silicon and their electrical effects. *Phys. stat. sol. (a)*, **78**, 527 - 538.
- /14/ Gleichmann R, Blumtritt H, Höpner A, Sullivan T (1991) Structural and electrical characterization of hot pressed grain boundaries in silicon by EBIC and TEM. *Polycrystalline Silicon II*, Springer Proceedings in Physics 54, Werner J H, Strunk H P (eds.), Springer-Verlag, 103 - 108.
- /15/ Graff K, Hefner H-A, Hennerici W (1988) Monitoring of internal gettering during bipolar processes. *J. Electrochem. Soc.* **135**, 952 - 957.
- /16/ Graff K (1989) Transition metals in silicon and their gettering behaviour. *Materials Science and Engineering* **B4**, 63 - 69.
- /17/ Heydenreich J, Blumtritt H, Gleichmann R, Johansen H (1981) Combined application of SEM (EBIC) and TEM for the investigation of the electrical activity of crystal defects in silicon. *Scanning Electron Microscopy*, 1981; I, 351 - 365.
- /18/ Hwang J M, Schröder D K (1986) Recombination properties of oxygen precipitated silicon. *J. Appl. Phys.* **59**, 2476 - 2487.
- /19/ Jakubowicz A, Habermeier H-U (1985) Electron-beam-induced current investigations of oxygen precipitates in silicon. *J. Appl. Phys.* **58**, 1407 - 1409.
- /20/ Kittler M (1980) On the characterization of electrically active inhomogeneities in semiconductor silicon by charge collection at Schottky barriers using the SEM-EBIC, (I) and (II). *Kristall und Technik* **15**, 185 - 192 and **15**, 575 - 584.
- /21/ Kittler M, Seifert W (1981) On the characterization of individual defects in silicon by EBIC. *Crystal Res. Technol.* **16**, 157 - 162.
- /22/ Kittler M, Seifert W (1981) On the sensitivity of the EBIC technique as applied to defect investigations in silicon. *Phys. stat. sol. (a)* **66**, 573 - 583.
- /23/ Kittler M, Bugiel E (1982) EBIC/TEM studies on the relation between electrical properties, crystallographic structure, and interaction with point defects of epitaxial stacking faults in silicon. *Crystal Res. Technol.* **17**, 79 - 89.
- /24/ Kittler M, Seifert W, Bugiel E, Richter H (1983) Characterization of dislocations and their effects in silicon device technology. *J. de Physique* **44**, C4-437 - C4-443.
- /25/ Kittler M, Schröder K W, Bugiel E, Becker C (1984) Quantitative EBIC investigations of bulk stacking faults in silicon. *Phys. stat. sol. (a)* **81**, K 131 - K 135.
- /26/ Kittler M, Seifert W, Schmalz K, Tittelbach-Helmrich K (1986) Comparison of EBIC and DLTS measurements on boron-doped CZ silicon contaminated with iron. *Phys. stat. sol. (a)* **96**, K 133 - K 137.
- /27/ Kittler M, Tillack B, Hoppe W, Seifert W, Banisch R, Richter H H, Rocher A (1988) EBIC investigations of thick SOI layers. *Rev. de Physique Appliquee* **23**, 281 - 288.
- /28/ Kittler M, Lärz J, Morgenstern G, Seifert W (1991) Characterization of polycrystalline silicon by EBIC. *J. de Physique IV*, **1**, C6-173 - C6-179.
- /29/ Kittler M, Seifert W (1991) Bright EBIC contrast of crystal defects in silicon. *Polycrystalline Silicon II*, Springer Proceedings in Physics 54, Werner J H, Strunk H P (eds.), Springer-Verlag, 96 - 102.
- /30/ Kittler M, Lärz J, Seifert W, Seibt M, Schröder W (1991) Recombination properties of structurally well defined NiSi₂ precipitates in silicon. *Appl. Phys. Lett.* **58**, 911 - 913.
- /31/ Kolbe M, Hollricher O, Gottschalk H, Alexander H (1989) Temperature dependent EBIC contrasts of grain boundaries and systems of dislocation loops in Si. *Inst. Phys. Conf. Ser.*, Inst. Physics - Bristol UK, **100**, 725 - 730.
- /32/ Leamy H J, Kimerling L C, Ferris S D (1976) Silicon single crystal characterization by SEM. *Scanning Electron Microscopy*, 529 - 538.
- /33/ Lee D M, Maher D M, Shimura F, Rozgonyi G A (1990) Misfit dislocation gettering and associated precipitation in Si/Si(Ge) epitaxial layers. *Semiconductor Silicon*, Huff H R, Barraclough K G, Chikawa J (eds.), *Electrochem. Soc. Proc. Vol. 90-7*, 639 - 650.
- /34/ Matare H F, Laakso C W (1969) Space-charge domains at dislocation sites. *J. Appl. Phys.* **40**, 476 - 482.
- /35/ Maurice J-L (1989) Electrical activity and impurity precipitation in silicon grain boundaries. *Solid State Phenomena*, Vols. **6 & 7**, 265 - 275.
- /36/ Maurice J L, Colliex C (1989) Fast diffusers Cu and Ni as the origin of electrical activity in a silicon grain boundary. *Appl. Phys. Lett.* **55**, 241 - 243.
- /37/ Pasemann L (1981) A contribution to the theory of the EBIC contrast of lattice defects in semiconductors. *Ultramicroscopy* **6**, 237 - 250.
- /38/ Pasemann L (1991) A contribution to the theory of beam induced current characterization of dislocations. *J. Appl. Phys.* **69**, 6387 - 6393.

/39/ Ravi K V, Varker C J, Volk C E (1973) Electrically active stacking faults in silicon. *J. Electrochem. Soc.* **120**, 533 - 541.

/40/ Seibt M, Graff K (1988) Characterization of haze-forming precipitates in silicon. *J. Appl. Phys.* **63**, 4444 - 4450.

/41/ Seibt M, Schröter W (1989) Precipitation behaviour of nickel in silicon. *Phil. Mag. A* **59**, 337 - 352.

/42/ Seibt M, Schröter W (1991) Formation and properties of metastable silicide precipitates in silicon. *Solid State Phenomena*, Vols. **19 & 20**, 283 - 294.

/43/ Seifert W, Kittler M (1987) Negative (bright) EBIC contrast at oxygen induced defects in silicon. *Phys. stat. sol. (a)* **99**, K11 - K14.

/44/ Shimura F (1989) *Semiconductor Silicon Crystal Technology*, Academic Press, chapter 5.3.

/45/ Sieber B (1989) Intrinsic or extrinsic origin of the recombination at extended defects. *Rev. de Physique Appliquee* **24**, C6-47 - C6-56.

/46/ Sieber B (1991) Experiments and theory of dislocations in GaAs. *Solid State Phenomena*, Vols. **19 & 20**, 353 - 365.

/47/ Sumino K (1989) Interaction of impurities with dislocations in semiconductors. *Point and Extended Defects in Semiconductors*, Benedek G, Cavallini A, Schröter W (eds.). NATO ASI Series, Ser. B: Physics Vol., Plenum - New York, **202**, 77 - 94.

/48/ Tarento R J, Mekki D E (1991) Influence of the depletion zone on EBIC charge collection imaging of localized defects in semiconductors. *Phys. stat. sol. (a)* **123**, 233 - 240.

/49/ Weber E R, Gilles D (1990) Transition metals in silicon: fundamentals and gettering mechanisms. *Semiconductor Silicon 1990*, Huff H R, Barraclough K G, Chikawa J (eds), *Electrochem. Soc. Proc. Vol.* **90-7**, 585 - 600.

/50/ Wilshaw P R, Fell T S, Booker G R (1989). Recombination at dislocations in silicon and gallium arsenide. *Point and Extended Defects in Semiconductors*, Benedek G, Cavallini A, Schröter W (eds.). NATO ASI Series, Ser B: Physics Vol., Plenum - New York, **202**, 243 - 256.

Discussion with Reviewers

C. Donolato: Don't you think that it would be more convenient not to include the minority-carrier diffusion coefficient into the definition of defect strength?

Authors: The definition of defect strength as given here is a question of convention and another definition is, of course, possible. Ideally, the defect strength should contain only parameters of the defect, not those of the surrounding material. So, one may argue not to include the minority-carrier diffusivity into γ , arriving then e. g. at an expression

$$\gamma = (4/3) \pi e^3 (1/\tau_d - 1/\tau)$$

instead of eq. (4) for a point-like defect. However, as γ contains the lifetime of the undisturbed material τ , this demand is still not completely met. Certainly, the proposed change of definition may have the advantage of providing a more obvious physical meaning of the defect strength. Namely, the dimension of γ will be equal then to:

$$\text{cm}^3\text{s}^{-1} \quad \text{for point-like defects,}$$

$$\text{cm}^2\text{s}^{-1} \quad \text{for line defects,}$$

$$\text{cm s}^{-1} \quad \text{for planar defects,}$$

see Donolato C (1989) Quantitative characterization of semiconductor defects by electron beam induced current. *Point and Extended Defects in Semiconductors*, Benedek G, Cavallini A, Schröter W (eds.). NATO ASI Series, Ser. B: Physics Vol. **202**, pp. 225 - 241.

In the case of a planar defect this is just the dimension of the well-known surface recombination velocity.

L. J. Balk: How does a changed microtopography increase the number of generated electron-hole pairs?

Authors: The microtopography causes changes of the energy deposition in the sample complementary to the variation of backscattered energy (visible as contrast in BSE images). Accordingly, when a certain microtopography results in reduced backscattering, the number of generated electron-hole pairs is increased and a bright EBIC contrast arises. Of course, the opposite is true for a microtopography giving rise to enhanced backscattering.

L. J. Balk: Can you give more detailed information in what sense the EBIC signal depends on the electrical field?

Authors: Supposition to obtain an EBIC signal is the existence of a sufficient electrical field separating the generated carriers. Under conditions of low injection the field of a junction is usually strong enough to collect practically all minority carriers generated in the SCR or reaching the SCR by diffusion. At high injection levels this may not be the case as the high carrier density may screen the electrical field, this way retarding the separation of carriers and increasing the probability of recombination in the junction SCR /32/. This effect will, of course, depend on the electrical field strength.

C. Donolato: In Fig. 10c the NiSi₂ precipitates are imaged as short segments. This suggests the absence of a depletion layer around them which seems to be present around those imaged in Fig. 10d. Which is the cause of this difference?

Authors: The contrasts in Fig. 10d are due to small, point-like defects with homogeneous depth distribution, whereas those in Fig. 10c are caused by

large elongated defects (10 ... 20 μm) located at the sample surface. The different appearance of the defects is related to differences both in beam energy and in habit and location of the defects.

A comparison of the activity of these defects is difficult as contrast mechanisms are probably different, due to the fact that the supposed SCR of the defect and the SCR of the junction may interfere, and because the theoretical modelling of contrast taking account of the junction SCR is still at the beginning.

R. Matson: In view of the excitation dependence of grain boundary recombination velocities (see, e. g. Sundaresan R, Fossum J G, Burk DE (1984) Demonstration of excitation-dependent grain-boundary recombination velocity in polycrystalline silicon. *J. Appl. Phys.* 56, 964), what exactly determined the use of 30 kV beam voltage for your experiments?

Authors: For reasons of applicability of existing contrast models the portion of carriers generated in the space-charge region of the surface Schottky junction used for charge collection should be as small as possible. This calls for large beam energies, but, on the other hand, low beam energies are necessary for good resolution. A beam energy of 30 keV is a reasonable compromise in our opinion.

A dependence of EBIC contrast on beam current is reported in the literature for different kinds of defects. Thereby, the factor governing the occurrence of this effect is rather not the excitation rate understood as number of carriers generated per second, but the density of generated carriers. Thus, it depends on both beam current and beam energy (extension of the generation region). In the paper referred to, experimental and theoretical EBIC profiles at GB's are given for $E_0 = 35$ keV, demonstrating a pronounced reduction of GB recombination velocity when increasing the excitation rate or when approaching the GB. For lower E_0 this behavior is expected to occur at lower excitation already, because of smaller extension of the generation region. Our experiments were carried out at excitation rates around and below $5 \cdot 10^{12} \text{ s}^{-1}$ ($E_0 = 30$ keV, $I_b < 100$ pA) and correspond to the case of 10^{13} s^{-1} excitation in the cited paper.

A. Jakubowicz: I suggest you to provide a more extended bibliography to raise the value of your article.

Authors: The different EBIC contrast and their underlying origin have been the subject of experimental and theoretical studies for a long time already. So, it is rather difficult to include a complete bibliography. Instead, besides references /32/ and /45/, we refer the reader interested in more detailed information to the following reviews and references therein:

Leamy H J, Kimerling L C, Ferris S D: Electron beam induced current. *Scanning Electron Microsc.* 1978; **1**, 717 - 726.

Hanoka J I, Bell R O: Electron-beam-induced currents in semiconductors. *Ann. Rev. Mater. Sci.* 1981; **11**, 353- 380.

Leamy H J: Charge collection scanning electron microscopy. *J. Appl. Phys.* 1982; **53**, R 51 - R 80.

Holt D B, Lesniak M: Recent developments in electrical microcharacterization using the charge-collection mode of the scanning electron microscope. *Scanning Electron Microsc.* 1985; **1**, 67 - 86.

Jakubowicz A: Theory of electron beam induced current and cathodoluminescence contrasts from structural defects of semiconductors. *Scanning Microscopy* 1987; **1**, 515- 533.

Holt D B: SEM Microcharacterization of Semiconductors. Holt D B and Joy D C (eds.), Academic Press 1989; chapter 6.

Concerning the discussion of whether EBIC contrast of defects is of intrinsic or extrinsic origin, the early work by Kawado et al. pointing to extrinsic origin should be emphasized:

Kawado S, Hayafuji Y, Adachi T: Observation of lattice defects in silicon using a new SEM-EBIC technique. *The Electrochem. Soc. 1975 Fall Meeting, Extended Abstracts* 1975; Vol. 75-2, No. 184.

Kawado S: Scanning electron microscopic observation of oxidation-induced stacking faults in silicon. *Jap. J. Appl. Phys.* 1980; **19**, 1591 - 1602.